Desalination and Water Treatment
www.deswater.com

doi: 10.1080/19443994.2015.1038738

57 (2016) 10664–10676
May

Taylor & Francis
Taylor & Francis Group

Effect of glutaraldehyde cross-linking degree of chitosan/sporopollenin microcapsules on removal of copper(II) from aqueous solution

İdris Sargin[a], Gulsin Arslan[b,*]

[a]*Faculty of Science, Department of Chemistry, Selcuk University, 42075 Konya, Turkey, Tel. +90 332 223 3887; Fax: +90 332 241 2499; email: idrissargin@hotmail.com*
[b]*Faculty of Science, Department of Biochemistry, Selcuk University, 42075 Konya, Turkey, Tel. +90 332 223 3852; Fax: +90 332 241 2499; email: 71arslan@gmail.com*

Received 23 July 2014; Accepted 29 March 2015

ABSTRACT

Bio-based sorbents, especially cross-linked chitosan, have been widely used in heavy metal removal. Type of cross-linking agent and degree of cross-linking largely affect metal sorption behaviour of chitosan-based sorbents. This study describes the preparation of chitosan/sporopollenin (CS) microcapsules cross-linked with different amount of glutaraldehyde (GA)/chitosan ratios. The microcapsules were modified by the incorporation of 0.3, 0.9 and 1.5 mL of GA solution (in water 25% v:v) for 1.50 g of chitosan. A protected cross-linking method was used for the preparation of the CS/GA microcapsules by the reaction of the microcapsules with Cu(II) as the protector. Scanning electron microscopy, Fourier transform infrared spectroscopy and thermogravimetric analysis were employed for the microcapsules characterization. The adsorption performance of the microcapsules was studied for the removal of Cu(II) at different concentration, contact time, amount of adsorbent, temperature and pH. The maximum Cu(II) removal values were 88.9, 100.4 and 80.7 mg g^{-1} by 0.3, 0.9 and 1.5 mL of GA impregnated CS microcapsules, respectively. The equilibrium adsorption isotherm data of the microcapsules exhibited a better fit to the Freundlich isotherm model. Affinity of the CS microcapsules for Zn(II), Cd(II), Ni(II) and Cr(III) in presence of Cu(II) was also investigated. GA/chitosan ratio affected the metal sorption performance and physicochemical properties of the microcapsules. The results revealed that CS microcapsules that were cross-linked with 0.9 mL of GA solution had better Cu(II) ion sorption capacity and can be cost-effective sorbents in water treatment.

Keywords: Adsorption; Chitosan; Sporopollenin; Microcapsule

1. Introduction

In many areas in the world, water bodies have been contaminated with heavy metal ions through discharge of industrial wastewater [1]. Many industrial activities, including mining drainage, smelting, metal finishing, metal surface treatment operations, plating, electrolysis, electric devices manufacturing, tannery operations, fertilizer and chemical production industries, are major source of heavy metal contamination [1–5]. Heavy metal ions are responsible from many health problems in humans as well as in animals and plants. Cu(II) ion, which is toxic and carcinogenic, is one of the heavy metals and has detrimental effects on

---

*Corresponding author.

living organisms [3]. Excessive ingestion can lead to health problems including liver damage, kidney failure, acute poisoning and gastrointestinal bleeding [1]. Studies aiming to remove Cu(II) ions effectively from wastewaters are needed.

Many techniques have been employed for heavy metal removal in wastewaters, such as membrane filtration, precipitation, chelation/complexation, ion-exchange, oxidation/reduction and adsorption. Each method has some advantages over the rest. However, adsorption is still the best option because it makes possible to use low-cost, sustainable, high-efficient and eco-friendly bioadsorbents with easy of recovery and reusability [1,6,7]. Materials with biological origin can make better adsorbents due to their non-toxicity, abundance and efficiency.

Sporopollenin is a bio-macromolecule and is found in the exine (outer skeleton) of moss and fern spores [8,9]. It is the most resistant component of spores [10] and highly resistant to biological decay, heat, mineral acid and alkaline treatments [11]. It is composed of mainly carotenoids and carotenoid esters [8,9]. Sporopollenin grains from *Lycopodium clavatum* (evergreen club moss) spores are easily extracted and can be harvested in large amounts. They exhibit excellent mechanical strength and monodispersity and constitute microcapsules with large cavities [12]. It has wider applications in many fields: food industry [13], chromatographic studies [14], dye removal [15] and heavy metal removal [16–18].

Chitosan, the deacetylated derivative of chitin, is a functional biopolymer with biodegradability, biocompatibility and high sorption capacity [19]. It can be physically and chemically modified in different forms: membranes [20], fibres [21], hydrogels [22], nanoparticles [23], beads [24], films [25] and capsules [26]. It has many applications in pharmaceutical [27], cosmetics [28], biotechnology [29], food industry [30] and water treatment [24]. In metal ion removal, it can be used in raw [31] or modified forms [32]. Also, in recent years, various chitosan composite sorbents have been synthesized with clay minerals [33], natural/biomaterials [34,35], magnetite [36], sand [37] and synthetic polymers [38]. However, in literature, there is no study on chitosan/sporopollenin (CS) composites.

Chitosan is soluble in acidic solutions and should be cross-linked to enhance its stability. Cross-linking makes chitosan not only mechanically stronger, but also more selective to some metal ions. Various cross-linking agents are used to cross-link the chitosan polymer, such as epichlorohydrin, ethyleneglycol diglycidyl ether, 1,1,3,3-tetramethoxypropane, β-cyclodextrin polyaldehyde or glutaraldehyde (GA). Free $-NH_2$ and –OH groups of chitosan polymer play a role in forming coordination complexes with metal ions. But, in case of cross-linking with GA, pendant $-NH_2$ groups on the chitosan polymer are involved in Schiff base formation, which in turn affects its interaction with metal ions by lowering the sorption sites on the polymer [39]. Wang et al. [40] recently reported that the amount of GA strongly affected Cu(II) adsorption onto chitosan/polyethylene glycol semi-interpenetrating polymer blend. They commented that higher GA dosages led to lower Cu(II) sorption capacity by decreasing number of pendant amino groups on chitosan polymer.

Incorporating fine biological macromolecules into the network of cross-linked chitosan can compensate for this loss by providing extra binding sites, selectivity and diffusion channels for metal ions. Earlier studies in the literature established the affinity of chitosan [39] and sporopollenin [14,16] for Cu(II) ions. Additionally, sporopollenin grains are monodisperse particles with desired size (20 μm) and large cavities. Considering these physical characteristics, using sporopollenin grains can be advantageous in production of chitosan-based biosorbents.

This is the first study reporting the preparation of GA cross-linked CS composite biosorbent with three different cross-linking degrees and its characterization by scanning electron microscopy (SEM), Fourier transform infrared (FT-IR) spectroscopy and thermo gravimetric analysis (TGA). The study also presents data on optimal amount of GA that is needed to cross-link the CS microcapsules. The study deals with the effect of chitosan/GA ratio on Cu(II) sorption capacity of the CS microcapsules and determines the affinity of the CS microcapsules for Zn(II), Cd(II), Ni(II) and Cr(III) in presence of Cu(II). The parameters (amount of sorbent, contact time, concentration, pH and temperature) effecting sorption Cu(II) capacity of the CS microcapsules were evaluated.

2. Experimental

2.1. Materials

Chitosan was received from BioLog (Biotechnology and Logistic GmbH) (in flake form with deacetylation degree of 85%, viscosity 2,500 mPa´s, ash content of <1%). Sporopollenin (*L. clavatum*) with 20 μm particle size was purchased from Fluka Chemicals. GA (25% in water v:v) and metal salts were obtained from Merck. All other chemicals (sodium hydroxide, acetic acid and methanol) were analytical grade and used without any treatment. De-ionized water (purified with ELGA DV 25 water purification system) was used to prepare the solutions. The metal solutions were prepared by diluting of the stock solution of 1.0 M.

2.2. Preparation of CS microcapsules

Chitosan (1.500 g) was dissolved in 150 mL of acetic acid solution (2% v:v) and stirred for 24 h. Then, sporopollenin grains (1.140 g) were mixed with the chitosan solution. After blending for 2 h, the mixture was transferred into a burette. The mix was dropped into coagulation solution (methanol–water–NaOH; 300 mL:200 mL:60 g) [22]. The microcapsules were incubated in the coagulation solution overnight to ensure the complete gelation. Then, the microcapsules were recovered and rinsed with water to neutral pH. Wet capsules were transferred into cross-linking reaction solution (GA solution in 60 mL of methanol) and refluxed at 70°C for 6 h. In this step, three different amounts of GA solutions were used: 0.3, 0.9 and 1.5 mL. The microcapsules obtained in each cross-linking procedure were named CSMCs1 (CS microcapsules), CSMCs2 and CSMCs3, respectively. The final product was rinsed with ethanol and then with water. Wet cross-linked microcapsules were left to dry at room temperature and kept in sealed containers.

2.3. Characterization of synthesized CSMCs

The surface characteristics of CSMCs were examined by employing EVO LS 10 ZEISS SEM. TGA of CSMCs was done with a Setaram Thermogravimetric Analyzer/Setsys (EXSTAR S11 7300). 15–17 mg of sample was used, and the analysis was carried out in argon atmosphere from room temperature to 900°C (gas flow rate: 20 mL min^{-1} and heating rate: 10°C min^{-1}). The IR spectra analysis was performed by a FT-IR spectrophotometer (Perkin Elmer100 FT-IR).

2.4. Batch adsorption experiments

The effects of metal concentration (in the range of 2–12 mg), pH of metal solution (i.e. 3.5, 4.5 and 5.6) and temperature (i.e. 25, 35 and 45°C) on adsorption equilibrium were investigated in 25 mL of Cu(II) solution at 200 rpm for 4 h. The microcapsules were separated by Whatman filter paper (No: 42). Cu(II) concentration in the solution was determined by an atomic absorption spectrometer (ContrAA 300, Analytikjena). The difference in Cu(II) ion concentration following the adsorption was calculated, and the amount of Cu(II) ions adsorbed per unit mass of the microcapsules was determined employing the equation below.

$$q_e = \frac{(C_i - C_e)V}{W} \tag{1}$$

where q_e is the metal sorption capacity of the CSMCs (mg g^{-1}); C_i and C_e are the initial and equilibrium liquid-phase concentrations of metal ions (mg L^{-1}), respectively; V is the volume of metal solution (L); and W is the mass of CSMCs used (g).

2.5. Sorption from binary mixtures

Binary mixtures composed of Cu(II)–Cr(III), Cu(II)–Zn(II), Cu(II)–Ni(II) and Cu(II)–Cd(II) were prepared and used in determining the order of binding ability of the metal ions to the CSMCs1, CSMCs2 and CSMCs3 adsorbents. In binary solutions, metal ion concentration was 10 mg L^{-1}, and pH was adjusted to 5.6 with dilute solutions of HCl and NaOH. The microcapsules (0.1 g) were placed into 25 mL of metal solutions and agitated at 200 rpm at 25°C for 4 h. The amounts of metal ions in the filtrate were determined with atomic absorption spectrometer.

2.6. Desorption in HCl and EDTA solutions

Desorption studies were performed in 25 mL of 0.1 M HCl and 0.1 M EDTA solutions. The Cu(II) loaded CSMCs were placed into HCl and EDTA solutions and agitated at 200 rpm at room temperature for 24 h. Then, the microcapsules were removed, and the filtrate was analysed. The percentage of desorption was determined using the expression given below:

$$\text{Desorption } (\%) = (m_d/m_a) \times 100 \tag{2}$$

where m_d is the amount of Cu(II) ions desorbed (mg L^{-1}) and m_a is the amount of Cu(II) ions adsorbed (mg L^{-1}). The final desorption % for each adsorbent is the average of two desorption studies.

3. Results and discussion

3.1. Characterization of synthesized CSMCs

3.1.1. Scanning electron microscope

Surface characteristics of CSMCs1, CSMCs2 and CSMCs3 microcapsules are depicted in the SEM images taken in different magnifications (Fig. 1). The figures confirm that entrapment of the sporopollenin

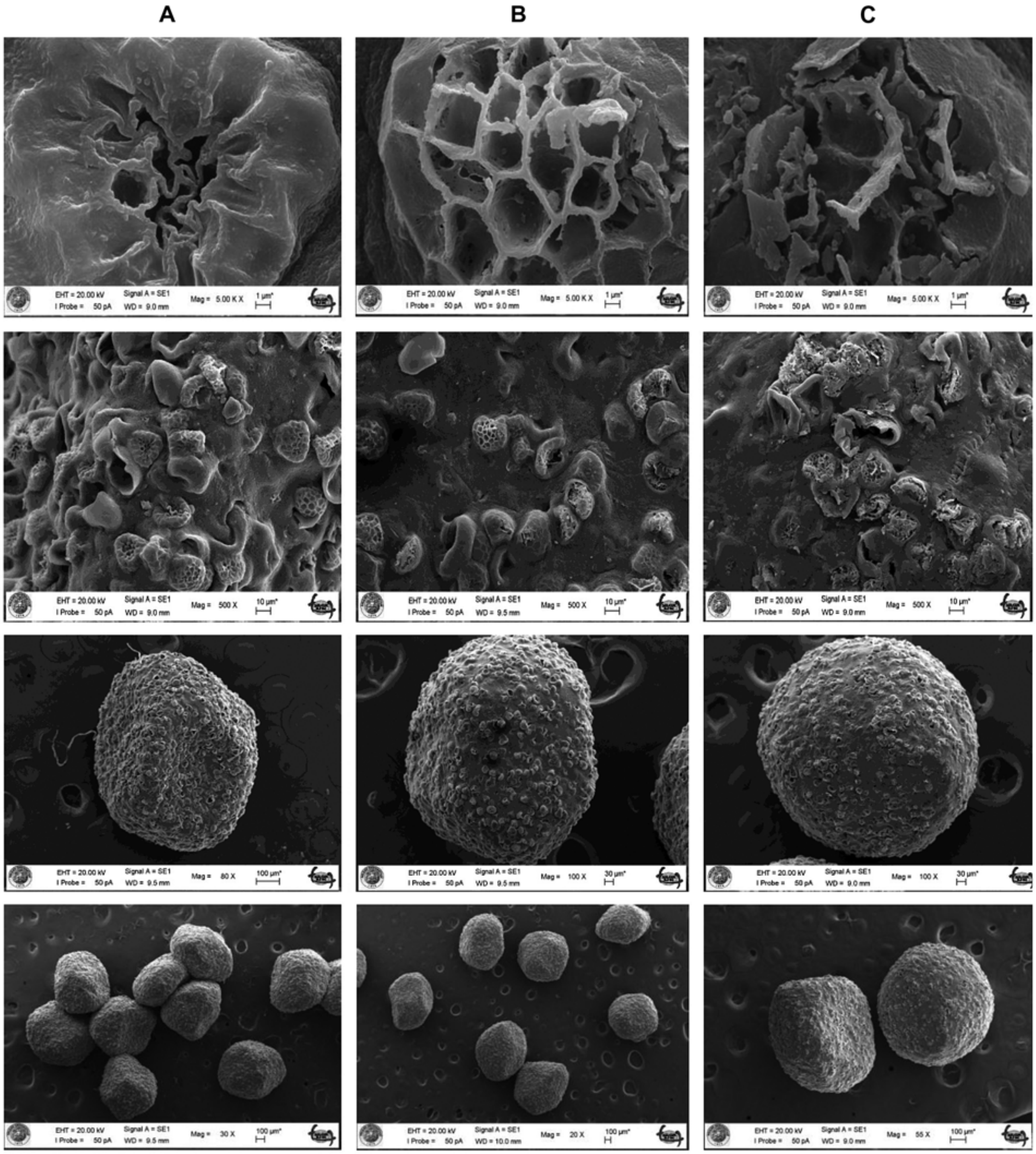

Fig. 1. SEM images of chitosan/sporopollenin microcapsules; CSMCs1 (A), CSMCs2 (B) and CSMCs3 (C).

grains was carried out successfully and they were embedded randomly in the polymer matrix. The images exhibit porous and rough surface morphology of the microcapsules. CSMCs3 microcapsule, which had the highest cross-linker/chitosan ratio, was more spherical in shape, and its surface was smoother, with less sporopollenin grains exposed to the surface.

During the synthesis, the microcapsules were subjected to chemical treatments: gelation in methanol–water–NaOH mixture and cross-linking in methanol–GA mixture. The effects of these treatments on sporopollenin grains can be seen in the SEM images. As presented in Fig. 1, although their surface morphologies were partially disrupted and the walls of the cavities were folded or destroyed, the grains could retain their structural integrity to some extent.

3.1.2. FT-IR analysis

The infrared spectra of the sporopollenin, chitosan and CSMCs are given in Fig. 2. Chitosan has a typical broad band (O–H and N–H stretching) at 3,293 cm^{-1}. In the spectrum of chitosan, the bands appearing at about 1,556 and 1,375 cm^{-1} could be assigned to the bending vibrations of N–H and C–H. The strong peak at 1,151 cm^{-1} can be corresponded to the C–O stretching. In the spectrum of raw sporopollenin, the band at 3,279 cm^{-1} is assigned to the stretching of –OH; the bands at 2,923 and 2,853 cm^{-1} to C–H; the band at 1,744 cm^{-1} to C=O; the band at 1,141 cm^{-1} to C–N stretching vibrations; and the one at 1,417 cm^{-1} to CH_2 and CH_3 groups [17]. The bands at around 1,655 and 1,417 cm^{-1} for –CO and –NH– groups were also observed. These observations in FT-IR spectra indicate the GA condensation onto chitosan polymer. In the spectra of CSMCs, the band observed at 1,741

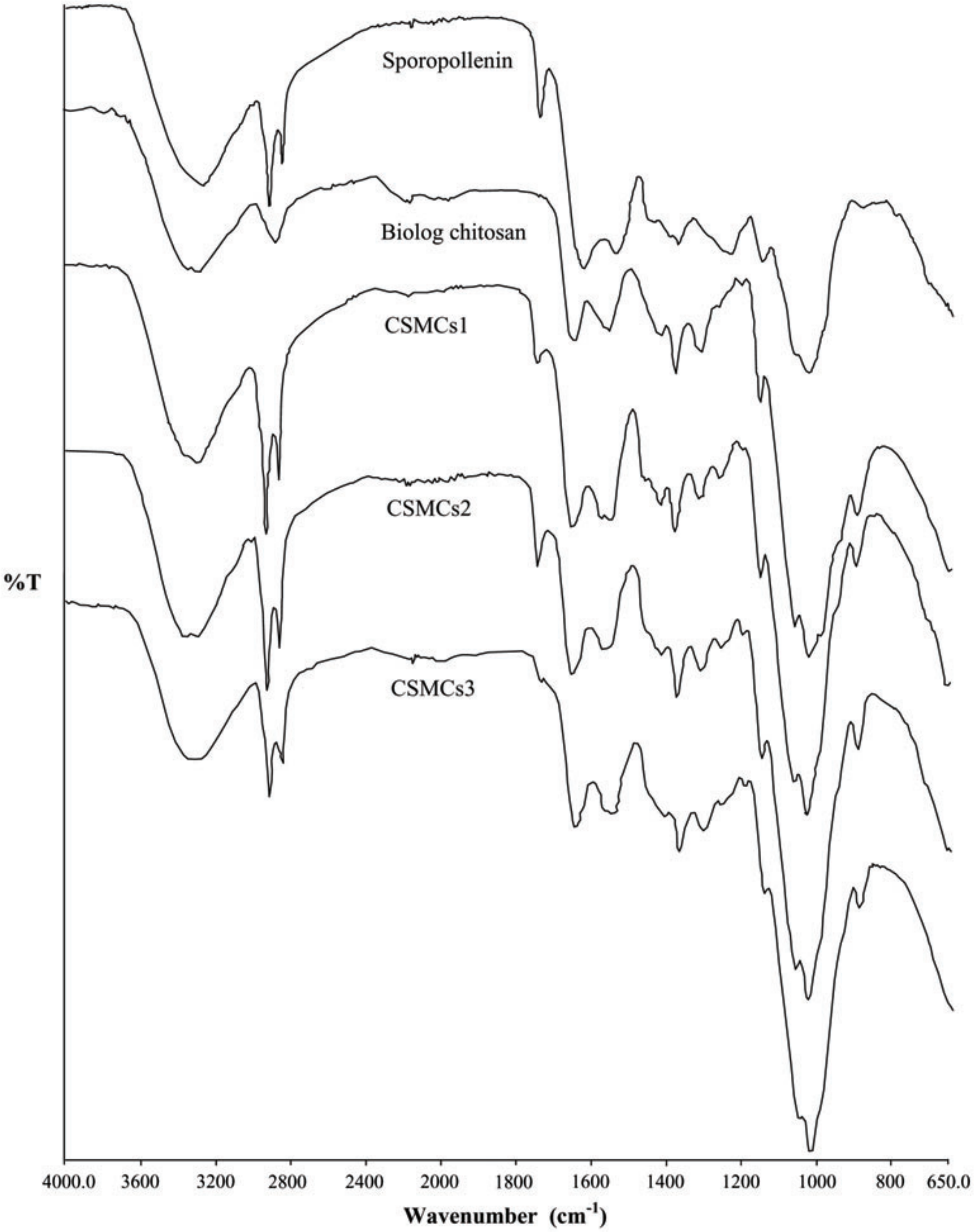

Fig. 2. FT-IR spectra of sporopollenin, chitosan and chitosan/sporopollenin microcapsules.

(CSMCs1), 1,743 (CSMCs2) and 1,743 cm^{-1} (CSMCs3) can be assigned to the stretching of carbonyl group of sporopollenin. The bands appearing at 1,648 (CSMCs1), 1,650 (CSMCs2) and 1,649 cm^{-1} (CSMCs3) can be attributed to imine (C=N) groups formed in via condensation of aldehydes of GA with $–NH_2$ groups of chitosan. Additionally, the bands at 1,579 (CSMCs1), 1,573 (CSMCs2) and 1,558 cm^{-1} (CSMCs3) can be corresponded to C–N stretching, and these bands can signify cross-linking of chitosan [41].

3.1.3. TGA

Chitosan is a highly crystalline polymer due to the strong intermolecular hydrogen bonds between its strands. Chemical modifications (i.e. imine formation via Schiff bases reaction) that disrupt these hydrogen bonds act on its crystallinity and also reduce its thermal stability [39,42]. Maximum decomposition temperature of chitosan has been reported to be 302˚C [43]. A gradually lower decomposition temperature for GA cross-linked chitosan is predicted as the GA/chitosan ratio increases. As for sporopollenin, a recent study by Fraser et al. [44] revealed that this macromolecule was heat resistant and its chemical structure did not alter until a threshold of 300˚C.

Three decomposition steps were observed in the thermograms of the CSMCs (Fig. 3). The first one (at around 110˚C) could be resulted from the evaporation of water molecules present within the polymeric network rather than degradation or decomposition of chitosan and sporopollenin. It seems that decomposition of cross-linked chitosan occurred in the second step at lower temperatures when compared to pristine chitosan. Mass losses in these steps were observed to be in the order of CSMCs3 > CSMCs2 > CSMCs1, representing the same trend as in GA/chitosan ratio of the CSMCs. On the other hand, the decomposition temperatures in the first and the second steps decreased as the GA/chitosan ratio increased. The last decomposition step could be attributed mainly to the degradation of heat-resistant sporopollenin grains. It appears that sporopollenin grains incorporated in the polymeric network did not contribute to the thermal

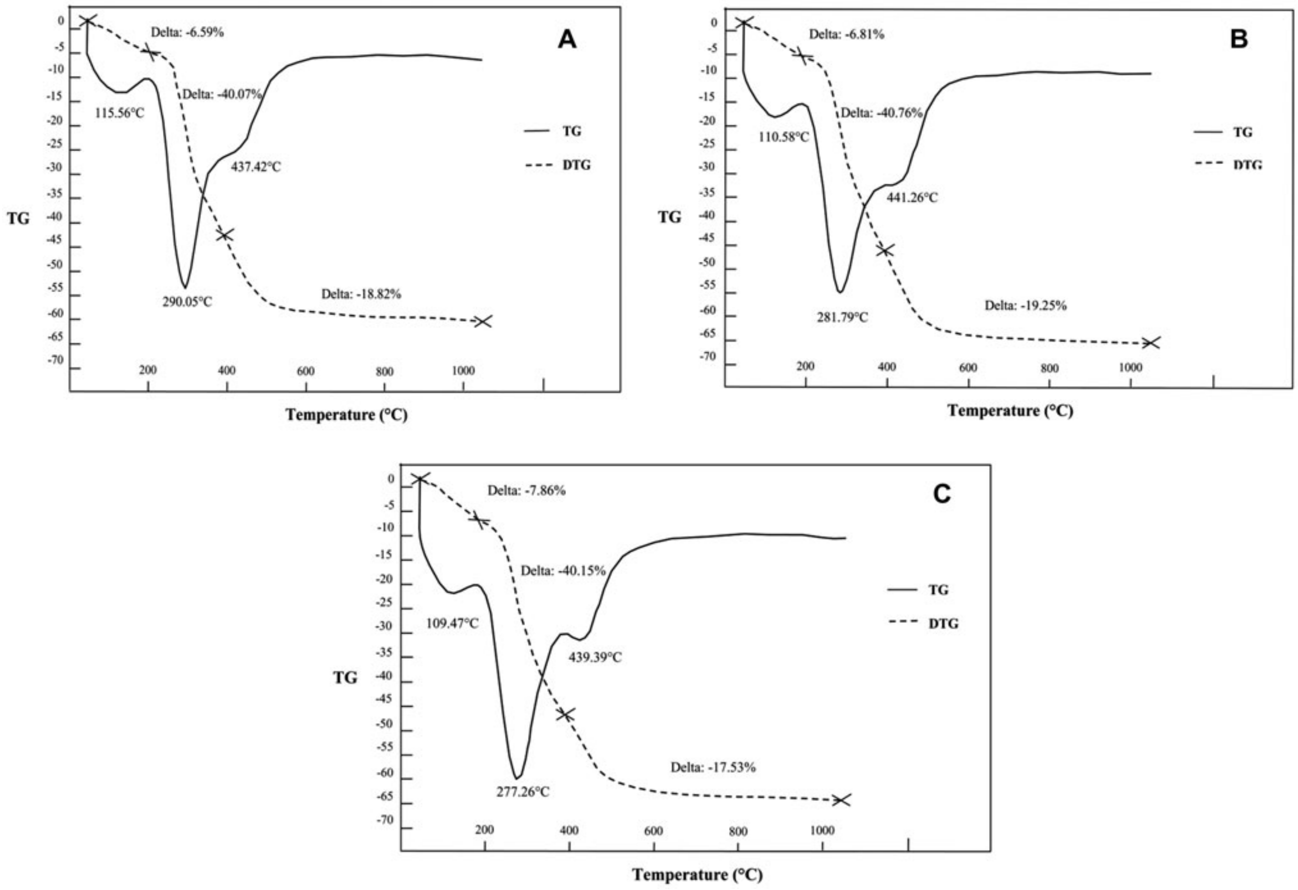

Fig. 3. TG-DTG curves of chitosan/sporopollenin microcapsules; CSMCs1 (A), CSMCs2 (B) and CSMCs3 (C).

stability of cross-linked chitosan. However, sporopollenin itself mainly decomposed at around ~440°C.

3.2. Batch adsorption experiments

3.2.1. Amount of adsorbent

The amount of adsorbent was studied in varying amounts of CSMCs1, CSMCs2 and CSMCs3 microcapsules (i.e. 0.0250–0.1500 g) (Fig. 4). Increase in the amount of the microcapsules led to higher percentage of Cu(II) ion removal at a certain point (~0.1000 g). After this point, increasing amount of the adsorbent did not significantly contribute to the percentage of the metal removal once sorption sites on the microcapsules were saturated [45]. It appeared that 0.1 g of microcapsules was sufficient for 25 mL of metal solution (dosage 4 g L^{-1}). This amount was not high when compared to the adsorbent dosages reported in the earlier literature. In a review study on copper ion removal from industrial wastewaters, Bilal et al. [1] compared the efficiency of biosorbents from various sources, and the authors listed adsorbent doses (in g L^{-1}) in wider ranges as follows: activated carbon with different origins, 0.1–25; fungal biomass, 0.2–15; algal biomass, 0.1–8; bacterial biomass, 0.2–32; yeasts biomass, 1–15; and agricultural/forest wastes adsorbents, 0.1–50 g L^{-1}.

It was observed that sorption equilibrium was achieved in lower dosages for CSMCs2 than CSMCs1 and CSMCs3, indicating its higher sorption efficacy. As reported in earlier studies, cross-linking of chitosan with GA reduced metal sorption capacity of chitosan sorbents [39,40]. Ngah and Fatinathan [45] synthesized chitosan–alginate composites sorbents for Cu(II) removal, and they used higher adsorbent dosage for chitosan–alginate beads cross-linked with GA (chitosan beads, 0.125, chitosan–GA 1:1 ratio beads, 0.200; and chitosan–GA 2:1 ratio beads, 0.500 g). However, here, the sorbent synthesized with the lowest GA amount did not have the highest sorption capacity. This can be attributed to the sporopollenin contents of the sorbents rather than the cross-linking ratio. As discussed in SEM analysis, CSMCs sorbents were composite materials with different size and shapes, showing the heterogeneous nature of the sorbents.

3.2.2. Effect of contact time

The effect of contact time was studied to determine the time required to reach the adsorption equilibrium (Fig. 5). In first 60 min, there was relatively rapid Cu (II) ion uptake for all the adsorbents. Equilibrium was attained nearly in 240 min for CSMCs1 and CSMCs2, but it took CSMCs3 about 240 min more time to reach the plateau value. This may be attributed to the physical features of the microcapsules (surface morphology, size and porosity). As discussed in Section 3.1.1, CSMCs3 microcapsules had less sporopollenin grains exposed to the surface and therefore less pores and less binding sites on them. As a result, Cu(II) ions needed more time to diffuse into CSMCs3 capsules. In an earlier study on copper ion sorption by sporopollenin grains [16], the sorption kinetics was fast and the equilibrium was reached within in the first 30 min. In another study [17], functionalized sporopollenin (first with 3-aminopropyltrimethoxysilane and then with GA) exhibited slower adsorption kinetics for copper ions, and the equilibrium was attained in 90 min.

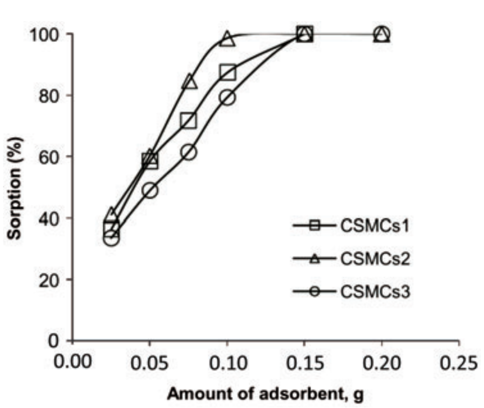

Fig. 4. Effect of adsorbent dosage on the sorption of Cu(II) by chitosan/sporopollenin microcapsules (initial concentration of Cu(II): 10 mg L^{-1}; pH of the solution: 5.6; temperature: 25 ± 1°C; shaking speed: 200 rpm).

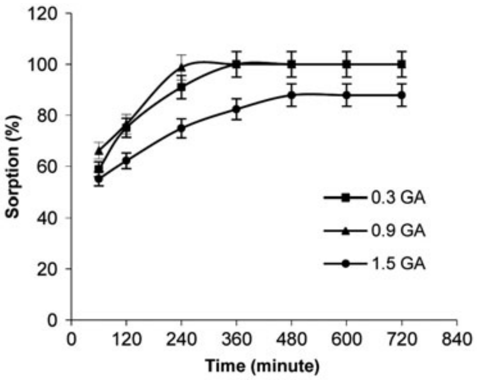

Fig. 5. Effect of contact time on the sorption of Cu(II) by chitosan/sporopollenin microcapsules (initial concentration of Cu(II): 10 mg L^{-1}; pH of the solution: 5.6; amount of CSMCs: 0.1000 g; temperature: 25 ± 1°C; shaking speed: 200 rpm).

It seems that sporopollenin grains entrapped in polymeric matrix show slower adsorption kinetics for copper ions. This can explain the longer contact time observed in this study.

3.2.3. Effect of pH

The effect of solution pH on Cu(II) ion removal was investigated at pH 3.5, 4.5 and 5.6 (Fig. 6). Maximum Cu(II) sorption was achieved at pH 5.6. Sorption studies could not be carried out at pH higher than 6.0 to avoid possible precipitation of copper hydroxide [40]. The amount of Cu(II) ion sorbed by the microcapsules was highly pH-dependent. Both metal ions and the corresponding adsorbent were greatly affected by alterations in the solution pH. Hydroxyl and amine functional groups on chitosan backbone were protonated at low pH, increasing positively charged adsorption sites on the adsorbent. This could lead to lower metal removal percentage because of the enhanced repulsion between the metal cations and the binding sites [37]. The CSMCs3 sorbent, the one with highest GA ratio, was less affected by the changes in pH when compared to the others. The cross-linking agent, GA, reacted with amino groups on chitosan via Schiff base formation and lowered the number of free amino groups. Therefore, CSMCs3 microcapsules had less free amino groups and exhibited a lower performance in Cu(II) removal. Other than amino groups, hydroxyl groups at the C-3 position on chitosan can interact with metal ions through electrostatic interaction and complexation [39]. On the other hand, the sporopollenin itself has polymeric nature, and the metal ion chelating moieties (aromatic, hydroxyl, carbonyl/carboxyl and ether functional groups) on it are also subject to protonation acidic medium. In an earlier study, the highest Cu(II) sorption on the sporopollenin grains occurred at pH 5.0 [16]. Another study reported Cu(II) ion adsorption on modified sporopollenin, and the author commented that higher the maximum adsorption was at pH 5.5 [17]. In a recent study by Wang et al. [40], the authors synthesized a semi-penetrating polymeric hydrogels with chitosan, and they observed that Cu(II) sorption capacity decreased at higher pHs as the GA/chitosan ratio was increased. The authors concluded that the swelling ratio of the hydrogels decreased at pH higher than 5, which in turn led to the reduction of internal volumes and Cu(II) sorption capacity. It seems that Cu(II) sorption on CSMCs has pH depending nature stemming from the cross-linking ratio of the microcapsules and its content, chitosan and sporopollenin.

3.2.4. Effect of temperature

Fig. 7 shows that Cu(II) uptake improved with the increase in the temperature for all three types of adsorbents. Cu(II) ion sorption percentage of CSMCs2 microcapsules increased about 2% (i.e. from 98.5 to 99.9%), but rising temperature enhanced the sorption capacity of CSMCs1 and CSMCs3 by around 13 and 11%. This observation may be explained by the expanding of channels/pores on the capsules with temperature and thus easier diffusion of Cu(II) ions through the pores. This could indicate more flexible and swelling nature of the least cross-linked one, CSMCs1 microcapsules.

Changes in standard free energy (ΔG°), enthalpy (ΔH°) and entropy (ΔS°) were calculated by plotting

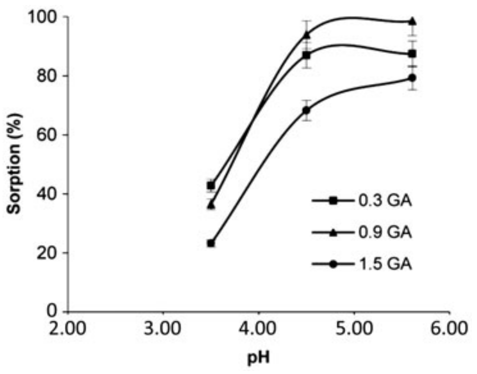

Fig. 6. Effect of pH on the sorption of Cu(II) by chitosan/sporopollenin microcapsules (initial concentration of Cu (II): 10 mg L^{-1}; contact time: 240 min; amount of CSMCs: 0.1000 g; temperature: 25 ± 1˚C; shaking speed: 200 rpm).

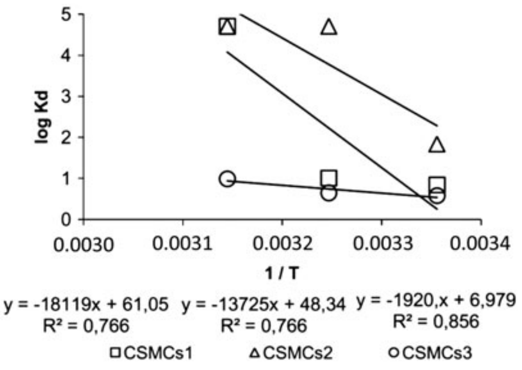

Fig. 7. Effect of temperature on the sorption of Cu(II) by chitosan/sporopollenin microcapsules (initial concentration of Cu(II): 10 mg L^{-1}; contact time: 240 min; pH of the solution 5.6; amount of CSMCs: 0.1000 g; shaking speed: 200 rpm).

log K_C vs. $1/T$ using the linear form of Van't Hoff equation.

$$\Delta G^\circ = -RT \ln K_C \tag{3}$$

$$\Delta G^\circ = \Delta H^\circ - T\Delta S^\circ \tag{4}$$

$$\log K_C = \frac{\Delta S^\circ}{2.303R} - \frac{\Delta H^\circ}{2.303RT} \tag{5}$$

where K_C is the equilibrium constant, R is universal gas constant, 8.314 J mol^{-1} K^{-1}, and T is the temperature (K). Thermodynamic parameters for the adsorption of Cu(II) on CSMCs1, CSMCs2 and CSMCs3 microcapsules were calculated (Table 1). The positive values of ΔH° indicated that the sorption of Cu(II) on the three microcapsule types was of endothermic nature. The negative values of change in ΔG° revealed that the sorption of Cu(II) onto the microcapsules was spontaneous and thermodynamically favoured for each temperature in studied conditions [16,17]. Further, as seen from the table, there was an increase in negative values of Gibbs free energy for each type of sorbents at higher temperatures. The positive value of ΔS° indicated the increased randomness at the system during the sorption, and this can be attributed to the replacement of adsorbed species by copper ions as suggested by some workers or release of water molecules coordinated to the metal cation [17]. However, in recent study, Liu and Lee reviewed copper ion adsorption studies with thermodynamic analysis and argued that further experimental studies on the thermodynamic parameters and surface chemistry should be done to reveal exact nature of the sorption [46].

3.2.5. Sorption from binary mixtures

Cu(II) sorption capacities of CSMCs1, CSMCs2 and CSMCs3 microcapsules in presence of competitive ions (Zn(II), Cd(II), Ni(II) and Cr(III)) were determined and are listed in Table 2. The copper ion adsorption capacity of the sorbents decreased in the binary mixtures when compared to that of in copper solutions: 88.9, 100.4 and 80.7 mg g^{-1}. In single-component Cu(II) solutions, CSMCs2 had the highest sorption capacity. However, in the presence of competitive ions, CSMCs1 exhibited better performance in Cu(II) sorption than CSMCs2 and CSMCs3. Cu(II) ion sorption capacities of the microcapsules were found to be in order of CSMCs1 > CSMCs2 > CSMCs3 in all the binary metal solutions. All the microcapsules showed higher affinity for Cu(II) ions over Cr(III), Zn(II), Cd(II) and Ni(II) ions in binary solutions. Ionic radius order of these ions is Cr(III) > Cd(II) > Zn(II) > Cu(II) > Ni(II). The number of accessible coordination sites formed within the polymeric matrix, ionic radius and the charge density of the ions could have a role in this behaviour.

3.2.6. Desorption studies and the reusability of the adsorbents

Desorption percentage of the Cu(II) ions in dilute HCl solution is significantly lower than that in chelating agent EDTA solution. Desorption in HCl solutions was found to be 3.88, 0.52 and 6.21% for the CSMCs1, CSMCs2 and CSMCs3, respectively. On the other, desorption of Cu(II) ions was more effective in EDTA solution: 84.27, 10.12 and 94.65%. The findings indicated that CSMCs1 and CSMCs3 can be regenerated in dilute EDTA solution.

3.3. Adsorption isotherms

The Langmuir model [47], Freundlich model [48] and Dubinin–Radushkevich (D–R) model [49] and Scatchard plot analysis [50] were employed to analyse the adsorption equilibrium data.

(1) The Freundlich model

$$\log q_e = \log K_F + \frac{1}{n} \log C_e \tag{6}$$

Table 1
Thermodynamic parameters for the adsorption of Cu(II) on chitosan/sporopollenin microcapsules

			ΔG° (J mol^{-1})		
Microcapsule type	ΔH° (J mol^{-1})	ΔS° (J K^{-1} mol^{-1})	T = 298.15 K	T = 308.15 K	T = 318.15 K
CSMCs1	346,944.4	1,168.992	−1,590.4	−13,280.3	−24,970.2
CSMCs2	262,807.7	925.619	−13,165.7	−22,421.9	−31,678.1
CSMCs3	36,764.4	133.635	−3,078.8	−4,415.2	−5,751.5

Table 2
Cu(II) sorption capacities of the chitosan/sporopollenin microcapsules in the presence of competitive ions (adsorbent dose: 0.1 g; temperature: 25˚C; pH: 5.6; volume of metal solution: 25 mL)

	mg g^{-1} Sorbent							
Microcapsule type	Cu(II)	Zn(II)	Cu(II)	Cd(II)	Cu(II)	Ni(II)	Cu(II)	Cr(III)
CSMCs1	79.1	18.9	74.7	14.6	78.5	6.69	80.4	42.3
CSMCs2	74.4	21.2	72.6	0.11	74.7	9.10	70.0	35.8
CSMCs3	62.1	14.2	59.7	25.9	59.2	5.99	53.2	26.2

where q_e, amount of solute adsorbed in mmol g^{-1}; C_e, the equilibrium concentration of the adsorbate in mM L^{-1}; and K_F and n, Freundlich constants denoting adsorption capacity and intensity of adsorption.

(2) The Langmuir model

$$\frac{C_e}{q_e} = \frac{C_e}{Q^0} + \frac{1}{Q^0 b} \tag{7}$$

where q_e, amount of solute adsorbed in mmol g^{-1}; C_e, the equilibrium concentration of the adsorbate in mmol L^{-1}; and Q^0 (in mmol g^{-1}) and b (in L $mmol^{-1}$), Langmuir constants related to adsorption capacity and energy of adsorption.

(3) The D–R model

$$\ln q_e = \ln X_m - K\varepsilon^2 \tag{8}$$

where ε (Polanyi Potential) is $[RT \ln(1 + (1/C_e))]$, q_e is the amount of the copper ions adsorbed per unit weight of microcapsules (mmol g^{-1}), X_m is the adsorption capacity (mmol g^{-1}), and K is a constant related to the adsorption energy in $mol^2\ kJ^{-2}$. The values of X_m and K were obtained from the intercept and slope of the lnq_e vs. ε^2 plots. By operating the K values in the equation below, the mean free energy of adsorption (E) was calculated:

$$E = (-2K)^{-0.5} \tag{9}$$

(4) The Scatchard plot analysis

$$q_e/C_e = K_s(Q_s - q_e) \tag{10}$$

where C_e, the equilibrium concentration of the adsorbate in mmol L^{-1}; q_e, equilibrium adsorbate capacity in mmol L^{-1}; and K_s (in L $mmol^{-1}$) and Q_s (in mmol g^{-1}) are the Scatchard isotherm constants.

Table 3 presents the parameters and correlation coefficients obtained from the plots of Freundlich (log q_e vs. log C_e), Langmuir (C_e/q_e vs. C_e) and D–R (ln q_e vs. ε^2) models and the Scatchard plot analysis (q_e/C_e vs. q_e).

When the regression coefficients in Table 3 are considered, it seems that sorption equilibrium of Cu (II) ions onto all the sorbents can be better explained by Freundlich isotherm model. The better fitting to Freundlich isotherm model indicated the heterogeneous nature of the microcapsules and the presence of the adsorption sites with differing energy. The values of $n > 1$ indicated the favourability of adsorption conditions [37]. Additionally, the deviation from linearity observed in the Scatchard plot analysis showed the presence of different types of the sorption sites on the microcapsules [51]. The mean free energy of adsorption, E values, obtained in D–R isotherm

Table 3
Parameters of Freundlich, Langmuir, Scatchard and D–R isotherms for sorption of Cu(II) ion on chitosan/sporopollenin microcapsules (adsorbent dose: 0.1 g; temperature: 25˚C; pH: 5.6; volume of Cu(II) solution: 25 mL)

	Freundlich isotherm			Langmuir isotherm			Scatchard isotherm			D-R isotherm			
Cu(II)	k	n	R^2	Q_0	b	R^2	K_s	Q_s	R^2	X_m	K	E	R^2
CSMCs1	1.959	7.576	0.838	1.142	126.839	0.654	75,648	0.141	0.562	1.379	0.001	22.361	0.784
CSMCs2	1.689	9.524	0.686	1.142	126.839	0.654	97,893	0.127	0.652	1.317	0.001	22.361	0.772
CSMCs3	1.396	9.804	0.894	0.910	50.551	0.617	12,736	1.092	0.686	1.099	0.001	22.361	0.867

model analysis, can provide information on the nature of the copper ion sorption, chemical, ion-exchange or physical adsorption. When E is higher than 16 kJ mol^{-1}, the nature of sorption can be considered to be chemisorption, whereas E values in a range of 8–16 kJ mol^{-1} show an ion-exchange mechanism, and if $E < 8$ kJ mol^{-1}, the sorption process is supposed to be of physical nature [52]. The higher E values (22.361 kJ mol^{-1}) for copper sorption by the microcapsules showed that the sorption proceeded most likely through chemisorption rather than ion-exchange mechanism or physisorption.

4. Conclusion

Chitosan polymer form complexes with metal ions mainly through free –NH_2 groups on the polymeric network. GA molecules cross-link chitosan polymer chains by forming Schiff base through these amino groups. Cross-linking procedure enhances chitosan capsules stability by lowering its solubility especially in acidic medium. On the other hand, decrease in the number of free amino groups of chitosan polymer greatly affects metal ion–chitosan interaction in metal removal studies. In this study, sporopollenin capsules were easily entrapped within the polymeric network of chitosan through cross-linking with GA. Cross-linking degree of the CS microcapsules affected the shape of the microcapsules and their Cu(II) sorption performance. The microcapsules (prepared with 1.500 g of chitosan and 1.14 g of sporopollenin and cross-linked with 0.9 mL of GA solution [25% aqueous solution, v:v]) exhibited better Cu(II) ion sorption performance than the microcapsules with 0.3 or 1.5 mL of GA solution. On the other hand, in the presence of competitive ions (Zn(II), Cd(II), Ni(II) and Cr(III)), all the three types of sorbent had higher affinity for Cu(II) ions, but the microcapsules cross-linked with 0.3 mL of GA solution had the highest Cu(II) sorption capacity. In further studies, heavy metal removal studies, various CS microcapsules can be prepared by manipulating sporopollenin/chitosan ratio or using chitosan with different molecular weight and deacetylation degree.

Acknowledgements

The authors are greatly indebted to the Selcuk University Research Foundation for providing a financial support (project number: BAP-14201082).

References

[1] M. Bilal, J.A. Shah, T. Ashfaq, S.M.H. Gardazi, A.A. Tahir, A. Pervez, H. Haroon, Q. Mahmood, Waste biomass adsorbents for copper removal from industrial wastewater—A review, J. Hazard. Mater. 263 (2013) 322–333.

[2] F. Mohammed-Azizi, S. Dib, M. Boufatit, Removal of heavy metals from aqueous solutions by Algerian bentonite, Desalin. Water Treat. 51 (2013) 4447–4458.

[3] N.A.A. Babarinde, J.O. Babalola, R.A. Sanni, Biosorption of lead ions from aqueous solution by maize leaf, Int. J. Phys. Sci. 1 (2006) 23–26.

[4] M.S. Rahman, M.R. Islam, Effects of pH on isotherms modeling for Cu(II) ions adsorption using maple wood sawdust, Chem. Eng. J. 149 (2009) 273–280.

[5] D.V. Quang, J.K. Kim, P.B. Sarawade, D.H. Tuan, H.T. Kim, Preparation of amino-functionalized silica for copper removal from an aqueous solution, J. Ind. Eng. Chem. 18 (2012) 83–87.

[6] A. Mellah, S. Chegrouche, M. Barkat, The removal of uranium(VI) from aqueous solutions onto activated carbon: Kinetic and thermodynamic investigations, J. Colloid Interface Sci. 296 (2006) 434–441.

[7] M. Kobya, Adsorption, kinetic and equilibrium studies of Cr(VI) by hazelnut shell activated carbon, Adsorpt. Sci. Technol. 22 (2004) 51–64.

[8] G. Bonhe, E. Richter, H. Woehlecke, R. Ehwald, Diffusion barriers of tripartite sporopollenin microcapsules prepared from pine pollen, Ann. Bot. 92 (2003) 289–297.

[9] E. Domínguez, J.A. Mercado, M.A. Quesada, A. Heredia, Pollen sporopollenin: Degradation and structural elucidation, Sex. Plant Reprod. 12 (1999) 171–178.

[10] J.S. Watson, W.T. Fraser, M.A. Sephton, Formation of a polyalkyl macromolecule from the hydrolysable component within sporopollenin during heating/pyrolysis experiments with *Lycopodium* spores, J. Anal. Appl. Pyrolysis 95 (2012) 138–144.

[11] B.P. Binks, J.H. Clint, G. Mackenzie, C. Simcock, C.P. Whitby, Naturally occurring spore particles at planar fluid interfaces and in emulsions, Langmuir 21 (2005) 8161–8167.

[12] M. Ersoz, E. Pehlivan, H.J. Duncan, S. Yildiz, M. Pehlivan, Ion exchange equilibria of heavy metals in aqueous solution on new chelating resins of sporopollenin, React. Polym. 24 (1995) 195–202.

[13] S. Barrier, A.S. Rigby, A. Diego-Taboada, M.J. Thomasson, G. Mackenzie, S.L. Atkin, Sporopollenin exines: A novel natural taste masking material, LWT – Food Sci. Technol. 43 (2010) 73–76.

[14] M. Erzengin, N. Ünlü, M. Odabaşı, A novel adsorbent for protein chromatography: Supermacroporous monolithic cryogel embedded with Cu^{2+}-attached sporopollenin particles, J. Chromatogr. A 1218 (2011) 484–490.

[15] A. Ayar, O. Gezici, M. Küçükosmanoğlu, Adsorptive removal of Methylene blue and Methyl orange from aqueous media by carboxylated diaminoethane sporopollenin: On the usability of an aminocarboxilic acid functionality-bearing solid-stationary phase in column techniques, J. Hazard. Mater. 146 (2007) 186–193.

[16] N. Ünlü, M. Ersoz, Adsorption characteristics of heavy metal ions onto a low cost biopolymeric sorbent from aqueous solutions, J. Hazard. Mater. 136 (2006) 272–280.

[17] I.H. Gubbuk, Isotherms and thermodynamics for the sorption of heavy metal ions onto functionalized sporopollenin, J. Hazard. Mater. 186 (2011) 416–422.

[18] M.A. Kamboh, M. Yilmaz, Synthesis of *N*-methylglucamine functionalized calix[4]arene based magnetic sporopollenin for the removal of boron from aqueous environment, Desalination 310 (2013) 67–74.

[19] R.A.A. Muzzarelli, J. Boudrant, D. Meyer, N. Manno, M. DeMarchis, M.G. Paoletti, Current views on fungal chitin/chitosan, human chitinases, food preservation, glucans, pectins and inulin: A tribute to Henri Braconnot, precursor of the carbohydrate polymers science, on the chitin bicentennial, Carbohydr. Polym. 87 (2012) 995–1012.

[20] G. Bayramoglu, M.Y. Yakup Arica, S. Bektas, Removal of Cd(II), Hg(II), and Pb(II) ions from aqueous solution using p(HEMA/chitosan) membranes, J. Appl. Polym. Sci. 106 (2007) 169–177.

[21] C.K.S. Pillai, W. Paul, C.P. Sharma, Chitin and chitosan polymers: Chemistry, solubility and fiber formation, Prog. Polym. Sci. 34 (2009) 641–678.

[22] A. Pal, S. Pan, S. Saha, Synergistically improved adsorption of anionic surfactant and crystal violet on chitosan hydrogel beads, Chem. Eng. J. 217 (2013) 426–434.

[23] Z. Wei, C. Wang, S. Zou, H. Liu, Z. Tong, Chitosan nanoparticles as particular emulsifier for preparation of novel pH-responsive Pickering emulsions and PLGA microcapsules, Polymer 53 (2012) 1229–1235.

[24] C.Y. Chen, T.H. Chang, J.T. Kuo, Y.F. Chen, Y.C. Chung, Characteristics of molybdate-impregnated chitosan beads (MICB) in terms of arsenic removal from water and the application of a MICB-packed column to remove arsenic from wastewater, Bioresour. Technol. 99 (2008) 748–794.

[25] N. Sharmin, R.A. Khan, D. Dussault, S. Salmieri, N. Akter, M. Lacroix, Effectiveness of silane monomer and gamma radiation on chitosan films and PCL-based composites, Radiat. Phys. Chem. 81 (2012) 932–935.

[26] M.N.V.R. Kumar, R.A.A. Muzzarelli, C. Muzzarelli, H. Sashiwa, A.J. Domb, Chitosan chemistry and pharmaceutical perspectives, Chem. Rev. 104 (2004) 6017–6084.

[27] I. Aranaz, M. Mengibar, R. Harris, I. Panos, B. Miralles, N. Acosta, G. Galed, A. Heras, Functional characterization of chitin and chitosan, Curr. Chem. Biol. 3 (2009) 203–230.

[28] S.Y. Ong, J. Wu, S.M. Moochhala, M.H. Tan, J. Lu, Development of a chitosan-based wound dressing with improved hemostatic and antimicrobial properties, Biomaterials 29 (2008) 4323–4332.

[29] O. Cota-Arriola, M.O. Cortez-Rocha, A. Burgos-Hernández, J.M. Ezquerra-Brauer, M. Plascencia-Jatomea, Controlled release matrices and micro/nanoparticles of chitosan with antimicrobial potential: Development of new strategies for microbial control in agriculture, J. Sci. Food Agric. 93 (2013) 1525–1536.

[30] F. Shahidi, R. Abuzaytoun, Chitin, chitosan, and co-products: Chemistry, production, applications, and health effects, Adv. Food Nutr. Res. 49 (2005) 93–135.

[31] N. Sankararamakrishnan, A.K. Sharma, R. Sanghi, Novel chitosan derivative for the removal of cadmium in the presence of cyanide from electroplating wastewater, J. Hazard. Mater. 148 (2007) 353–359.

[32] Y. Vijaya, S.R. Popuri, V.M. Boddu, A. Krishnaiah, Modified chitosan and calcium alginate biopolymer sorbents for removal of nickel (II) through adsorption, Carbohydr. Polym. 72 (2008) 261–271.

[33] Y. Peng, D. Chen, J. Ji, Y. Kong, H. Wan, C. Yao, Chitosan-modified palygorskite: Preparation, characterization and reactive dye removal, Appl. Clay Sci. 74 (2013) 81–86.

[34] K. Yu, J. Ho, E. McCandlish, B. Buckley, R. Patel, Z. Li, N.C. Shapley, Copper ion adsorption by chitosan nanoparticles and alginate microparticles for water purification applications, Colloids Surf., A 425 (2013) 31–41.

[35] H. Liu, F. Yang, Y. Zheng, J. Kang, J. Qu, J.P. Chen, Improvement of metal adsorption onto chitosan/*Sargassum* sp. composite sorbent by an innovative ion-imprint technology, Water Res. 45 (2011) 145–154.

[36] H.V. Tran, L.D. Tran, T.N. Nguyen, Preparation of chitosan/magnetite composite beads and their application for removal of Pb(II) and Ni(II) from aqueous solution, Mater. Sci. Eng. 30 (2010) 304–310.

[37] M.W. Wan, C.C. Kan, B.D. Rogel, M.L.P. Dalida, Adsorption of copper (II) and lead (II) ions from aqueous solution on chitosan-coated sand, Carbohydr. Polym. 80 (2010) 891–899.

[38] V. Janaki, B.T. Oh, K. Shanthi, K.J. Lee, A.K. Ramasamy, S. Kamala-Kannan, Polyaniline/chitosan composite: An eco-friendly polymer for enhanced removal of dyes from aqueous solution, Synth. Met. 162 (2012) 974–980.

[39] E. Guibal, Interactions of metal ions with chitosan-based sorbents: A review, Sep. Purif. Technol. 38 (2004) 43–74.

[40] M.-Q. Wang, J. Yan, S.-G. Du, J.-W. Zeng, W.-P. Chang, Y. Guo, H.-G. Li, Adsorption characteristic of copper ions and its application in electroless nickel plating on a hydrogel-functionalized poly(vinyl chloride) plastic, J. Mater. Sci. 48 (2013) 7224–7237.

[41] G.D. Altun, S.A. Cetinus, Immobilization of pepsin on chitosan beads, Food Chem. 100 (2007) 964–971.

[42] F.A.A. Tirkistani, Thermal analysis of some chitosan Schiff bases, Polym. Degrad. Stab. 60 (1998) 67–70.

[43] M. Kaya, T. Baran, A. Mentes, M. Asaroglu, G. Sezen, K.O. Tozak, Extraction and characterization of α-chitin and chitosan from six different aquatic invertebrates, Food Biophys. 9 (2014) 145–157.

[44] W.T. Fraser, J.S. Watson, M.A. Sephton, B.H. Lomax, G. Harrington, W.D. Gosling, S. Self, Changes in spore chemistry and appearance with increasing maturity, Rev. Palaeobot. Palynol. 201 (2014) 41–46.

[45] W.S.W. Ngah, S. Fatinathan, Adsorption of Cu(II) ions in aqueous solution using chitosan beads, chitosan–GLA beads and chitosan–alginate beads, Chem. Eng. J. 143 (2008) 62–72.

[46] X. Liu, D.-J. Lee, Thermodynamic parameters for adsorption equilibrium of heavy metals and dyes from wastewaters, Bioresour. Technol. 160 (2014) 24–31.

[47] I. Langmuir, The adsorption of gases on plane surfaces of glass, mica and platinum, J. Am. Chem. Soc. 40 (1918) 1361–1403.

[48] H. Freundlich, Ueber die Adsorption in Loesungen, Z. Physik. Chem. 57 (1907) 385–470.

[49] M.M. Dubinin, L.V. Radushkevich, The equation of the characteristic curve of the activated charcoal, Proc. Acad. Sci. USSR, Phys. Chem. Sect. 55 (1947) 331–337.

[50] R.H. Crist, J.R. Martin, D. Carr, J.R. Watson, H.J. Clarke, Interaction of metals and protons with algae. 4. Ion exchange vs adsorption models and a reassessment of Scatchard plots; ion-exchange rates and equilibria compared with calcium alginate, Environ. Sci. Technol. 28 (1994) 1859–1866.

[51] M. Küçükosmanoğlu, O. Gezici, A. Ayar, The adsorption behaviors of Methylene Blue and Methyl Orange in a diaminoethane sporopollenin-mediated column system, Sep. Purif. Technol. 52 (2006) 280–287.

[52] M. Tuzen, A. Sarı, Biosorption of selenium from aqueous solution by green algae (*Cladophora hutchinsiae*) biomass: Equilibrium, thermodynamic and kinetic studies, Chem. Eng. J. 158 (2010) 200–206.